Proceedings of the ASME 2013 International Design Engineering Technical Conferences & Computers and Information in Engineering Conference
IDETC/CIE 2013
August 4-7, 2013, Portland, Oregon, USA

13257

APPLICATION OF VISCOUS AND IWAN MODAL DAMPING MODELS TO EXPERIMENTAL MEASUREMENTS FROM BOLTED STRUCTURES

Brandon J. Deaner
Graduate Research Assistant
Department of Engineering Physics
University of Wisconsin-Madison
534 Engineering Research Building
1500 Engineering Drive
Madison, Wisconsin 53706
bdeaner@wisc.edu

Matthew S. Allen
Assistant Professor
Department of Engineering Physics
University of Wisconsin-Madison
535 Engineering Research Building
1500 Engineering Drive
Madison, Wisconsin 53706
msallen@engr.wisc.edu

Michael J. Starr
Component Science and Mechanics
Sandia National Laboratories
P.O. Box 5800
Albuquerque, NM, 87185
mjstarr@sandia.gov

Daniel J. Segalman
Multi-Physics Modeling & Simulation Department
Sandia National Laboratories
P.O. Box 969, Mail Stop 9042
Livermore, CA, 94551
djsegal@sandia.gov

ABSTRACT

Measurements are presented from a two-beam structure with several bolted interfaces in order to characterize the nonlinear damping introduced by the joints. The measurements (at force levels below macro-slip) reveal that each underlying mode of the structure is well approximated by a single degree-of-freedom system with a nonlinear mechanical joint. At low enough force levels the measurements show dissipation that scales as the second power of the applied force, agreeing with theory for a linear viscously damped system. This is attributed to linear viscous behavior of the material and/or damping provided by the support structure, which simulates free-free boundary conditions. At larger force levels the damping is observed to behave nonlinearly, suggesting that damping from the mechanical joints is dominant. A model is presented that captures these effects, consisting of a spring and viscous damping element in parallel with a 4-Parameter Iwan model. The parameters of this model are identified for each mode of the structure and comparisons suggest that the model captures the linear and nonlinear damping accurately over a range of forcing levels.

INTRODUCTION

Mechanical joints are known to be a major source of damping in assembled structures. However, the amplitude dependence of damping in mechanical joints has proven to be quite difficult to predict. For many systems, linear damping models seem to capture the response of a structure near the calibrated force level, but the damping may increase by an order of magnitude or more as the response level increases, leading to over-conservative designs. On the other hand, many of these structures still seem to exhibit the same uncoupled linear modes that were evident at low amplitudes. This work seeks to develop a model that is valid over a range of force levels and captures this variation in damping, while preserving much of the simplicity of the linear model.

Mechanical joints are said to be undergoing micro-slip when the joint as a whole remains intact but small slip displacements occur at the outskirts of the contact patch causing frictional energy loss in the system [1]. When this is the case the overall response of the structure is often well approximated with a linear since the stiffness and mass are not significantly changed, yet the damping may change significantly. The 4-Parameter Iwan model developed by

Segalman [2] captures these effects and has been shown to reproduce the behavior of real lap joints as observed in an extensive testing and modeling campaign [1], including the power law energy dissipation seen in the micro-slip region. In the past decade, the 4-Parameter Iwan model has been implemented to predict the vibration of structures with a few discrete joints [3, 4]. However, when modeling individual joints, each joint may require a unique set of parameters, which means that one must deduce hundreds or even thousands of joint parameters to describe a system of interest. On the other hand, when a small number of modes are active in a response, recent measurements have suggested that a simpler model may be adequate. Segalman et al. recently applied the 4-Parameter Iwan model in a modal framework to describe both discrete joint simulations and experimental data from structures with bolted joints [5, 6].

This work extends the modal Iwan framework adding some features that are necessary to approximate real experimental data. The 4-Parameter Iwan model only accounts for the energy dissipation associated with the mechanical joints of the system, which dominate at large force levels. However, at low force levels, the damping of the system is dominated by material damping of the structure and damping from the suspension support conditions of the experimental set-up. These linear sources of damping must be accounted for when fitting experimental data. In this work, the linear modal damping will be accounted for using a viscous damper in parallel with the 4-Parameter Iwan modal model. Experimental measurements are presented and are found to be well represented by this model.

The following sections review the Modal Iwan Modeling framework proposed by Segalman and discuss an experimental approach that can be used to deduce the modal Iwan parameters from measurements. These ideas are then applied to an assembly of two beams that are joined by four lap joints and found to reproduce the behavior of the first several modes quite adequately.

NOMENCLATURE

q_0	Modal amplitude of displacement
F_{VD}	Force in the viscous damper
C	Modal viscous damping coefficient
F_{LE}	Force in the linear elastic spring
K_∞	Linear elastic stiffness of the system
F_{Iwan}	Force in the Iwan joint
R, χ	Coefficient and exponent in the Iwan distribution function
F_S	Force necessary to cause macro-slip of joint
K_T	Stiffness of the Iwan joint
β	Iwan parameter related to level of energy dissipation and shape of energy dissipation curve
D_{Model}	Energy dissipated by the model
K_{Model}	Stiffness of the model
V(t)	Analytic signal
KE	Kinetic Energy
D_{Exp}	Energy dissipated by experimental data
K_{Exp}	Stiffness of the experimental data
f	Total optimization objective function
f_D	Energy dissipation objective function
f_K	Stiffness objective function

MODAL MODEL

Segalman proposed that nonlinear energy dissipation due to bolted joints could be applied on a mode-by-mode basis, using a 4-parameter Iwan constitutive model for each mode [5]. In general, the nonlinearity that joints introduce can couple the modes of a system so that modes in the traditional linear sense can not be defined. However, damping is often a relatively weak effect and experiments have often shown that the modes of structures with joints are typically quite linear and uncoupled. This suggests that one might be able to model the structure as a collection of uncoupled linear modes, each with nonlinear damping characteristics [6], and this is precisely the approach adopted in this work.

Under these assumptions, each modal degree-of-freedom is modeled by a single degree-of-freedom oscillator, as shown in Fig. 1, with a 4-parameter Iwan model in parallel with a viscous damper and an elastic spring. Note that the displacement of the mass is not a physical displacement but the modal displacement or modal amplitude, q, of the mode of interest. The mode vectors are assumed mass normalized so the mass is taken to be unity.

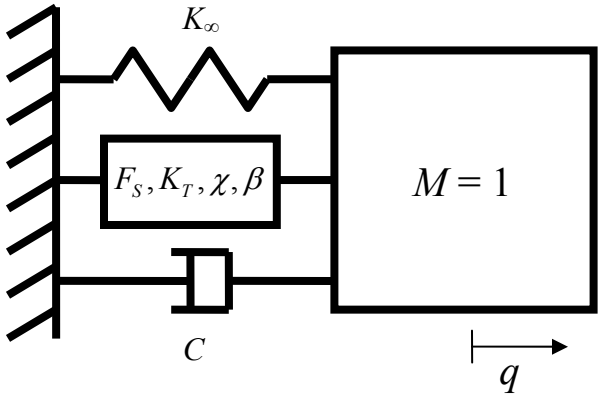

Fig. 1 Schematic of the model for each modal degree of freedom. Each mode has a unique set of Iwan parameters that characterize its nonlinear damping and a viscous damper that captures the linear component of the damping.

The 4-parameter Iwan model has parameters $\{F_S, K_T, \chi, \beta\}$ where F_S is the joint force necessary to initiate macro-slip, K_T is the stiffness of the joint, χ is directly related to the slope of the log energy dissipation versus log modal force in the micro-slip regime, and β relates to the level of energy dissipation and the shape of the energy dissipation curve as the macro-slip force is approached. Finally, the viscous damper has a coefficient, C,

and the linear elastic spring stiffness is K_∞. Note that all of the parameters are defined in modal and not physical space.

ENERGY DISSIPATION AND STIFFNESS

Model

The energy dissipation for the modal model seen in Fig. 1 can be solved for and used to fit experimental data. Assuming a harmonic load is applied to the mass and the system is at steady-state, the mass will oscillate as

$$q = q_0 \sin(\omega t) \tag{1}$$

where q_0 is the modal displacement amplitude and ω is the response frequency. The force in the viscous damper can be written as

$$F_{VD} = C\dot{q} \tag{2}$$

where C is the viscous damping coefficient. The force in the linear elastic spring takes the form

$$F_{LE} = K_\infty q \tag{3}$$

where K_∞ is the spring stiffness. The force in the Iwan joint is given in [2]. Assuming that the amplitude of motion is small, $q_0 < \phi_{\max}$ or in other words the Iwan joint is undergoing micro-slip, the force in the Iwan model can be approximated as

$$F_{Iwan} = \frac{Rq^{\chi+2}}{\chi+2} \tag{4}$$

where R is a coefficient that describes the population distribution of the parallel-series Iwan system [2]. These forces can be added, $F_{Total} = F_{VD} + F_{LE} + F_{Iwan}$, multiplied by the modal velocity and integrated over one period as follows,

$$D_{Model} = \int_0^{\frac{2\pi}{\omega}} F_{Total}\dot{q}\, dt \tag{5}$$

to obtain the energy dissipation per cycle, D_{Model}.

$$D_{Model} \approx \frac{4Rq_0^{\chi+3}}{(\chi+3)(\chi+2)} + \pi\omega C q_0^2 \tag{6}$$

Notice that the energy dissipation depends on the maximum modal amplitude q_0 and that the linear elastic spring does not contribute to the energy dissipated as one would expect.

From [2], the secant stiffness of the Iwan joint at large amplitudes of oscillation can be approximated as:

$$K_{Model} \approx K_T\left(1 - \frac{r^{\chi+1}}{(\chi+2)(\beta+1)}\right) + K_\infty \tag{7}$$

where

$$r = \frac{q_0 K_T\left(\beta + \frac{\chi+1}{\chi+2}\right)}{F_S(1+\beta)} \tag{8}$$

Note that both D_{Model} and K_{Model} as presented above are approximations to the actual dissipation and stiffness, and are valid in the micro-slip regime only. In order to obtain the actual dissipation and stiffness, the Iwan model can be integrated in time and then the actual dissipation and stiffness can be deduced. However, as discussed in later sections, these simple expressions for D_{Model} and K_{Model} are used to decrease computational time when solving an optimization problem to find the modal Iwan parameters that best fit the data.

Processing Experimental Measurements

The energy dissipation for each mode of a system can be computed from measurements of its free response. The procedure for processing measurements was presented in [6] and will be reviewed briefly below.

First, a filter is used to isolate an individual modal response. The authors have used both modal filters [7] and standard, infinite impulse response band-pass filters [8] for this purpose and other possibilities certainly exist. The Hilbert Transform [9] is then used to compute the instantaneous damping and frequency of the system. This process requires some care since the basic Hilbert transform performs very poorly in the presence of noise. This work uses a variant [10] where a polynomial is fit to smooth the instantaneous amplitude and phase found by a standard Hilbert transform and then the curve fit model can be differentiated to estimate the instantaneous frequency, as explained below.

One obtains an analytic representation of the modal response, denoted $V(t)$, by adding the Hilbert transform of the modal velocity, $\tilde{v}(t)$, to the measured modal velocity of the mode of interest, $v(t) = \dot{q}_r(t)$ as follows

$$V(t) = v(t) + i\tilde{v}(t) \tag{9}$$

The magnitude of the analytic signal is the decay envelope of the response and is approximated by

$$\left|V(t)\right| = V_0\, \mathrm{e}^{P(t)} \tag{10}$$

where V_0 is the initial amplitude. To maintain similarity with a linear system, the product of the natural frequency, $\omega_n(t)$, and the coefficient of critical damping, $\zeta(t)$, is defined to be the time derivative of $P(t)$.

$$\frac{dP(t)}{dt} = \alpha(t) \triangleq -\zeta(t)\omega_n(t) \tag{11}$$

The instantaneous phase is the complex angle of the analytic signal, which can be obtained using the following (provided that a four-quadrant arctangent formula is used).

$$\varphi(t) = \tan^{-1}\left(\frac{\tilde{v}(t)}{v(t)}\right) \tag{12}$$

The measured phase and the natural logarithm of the decay envelope are then smoothed by fitting a polynomial to the data. In addition, before the data is fit, the beginning and end of the data are deleted since they tend to be contaminated by end effects in the Hilbert Transform. The time-derivative of the phase then gives the instantaneous damped natural frequency.

$$\omega_d(t) = \frac{d\varphi(t)}{dt} \tag{13}$$

The time varying natural frequency is then found using the following equation:

$$\omega_n(t) = \sqrt{\left(\omega_d(t)\right)^2 + \left(-\alpha(t)\right)^2} \tag{14}$$

Now the energy dissipation per cycle can be calculated from the change in kinetic energy over one cycle. The amplitude of the kinetic energy can be written as,

$$KE = \frac{1}{2} M \left|V(t)\right|^2 \tag{15}$$

and the change in the kinetic energy is found by taking the derivative of this expression. Since the kinetic energy and its derivative are quite smooth, the energy dissipated per cycle, D_{Exp}, can be approximated by simply multiplying *dKE/dt* by the period ($2\pi/\omega_n(t)$) (e.g. using a trapezoid rule to integrate the power dissipated as a function of time).

$$D_{Exp} \approx \frac{2\pi}{\omega_d}\frac{dKE}{dt} = \frac{2\pi}{\omega_d}\frac{dP(t)}{dt}\left|V(t)\right|^2 \tag{16}$$

Finally, the experimental modal stiffness is simply the square of the time varying natural frequency.

$$K_{Exp} = \omega_n(t)^2 \tag{17}$$

The parameters, $\{F_S, K_T, K_\infty, \chi, \beta\}$, of the modal Iwan model can be found using a graphical approach as described in [6]. First, the experimental energy dissipated per cycle, D_{Exp}, and stiffness, K_{Exp}, are obtained using a Hilbert transform as described in [11]. The energy dissipation per cycle and stiffness can then be plotted versus the modal acceleration $\ddot{q}$, and since the mode shapes are mass normalized this is equal to the modal force. The χ parameter is found by fitting a line to the data for the log of energy dissipation versus log of the modal force at low force levels. Then the χ parameter for each mode *r* is given by:

$$\chi_r = \text{Slope}_r - 3 \tag{18}$$

In order to deduce the modal Iwan stiffness, K_T, the natural frequencies of each mode are plotted versus modal joint force. A softening of the system, characterized by a drop in frequency, illustrates the amount of modal stiffness associated with all the relevant joints of the system. The equation for modal joint stiffness for each mode becomes

$$K_{T,r} = K_{0,r} - K_{\infty,r} = \omega_{0,r}^2 - \omega_{\infty,r}^2 \tag{19}$$

where ω_0 is the natural frequency corresponding to the case when all the joints in the structure exhibit no slipping, and ω_∞ is the natural frequency when all of the joints are slipping. However, macro-slip was not clearly observed at the force levels tested so ω_∞ values were simply assumed to be slightly lower than the lowest observed natural frequency.

The modal joint slip force, F_S, can be estimated from the modal force level at which the stiffness or frequency begins to drop. To find the last parameter, β, all of the previous parameters found are needed along with the y-intercept, A_r, of the line that was fit in order to find χ_r. Then, the following equation from [2] can be used to solve for β_r numerically.

$$F_{S,r} = \left[\frac{4\left(\chi_r+1\right)K_{T,r}^{\chi_r+2}\left(\beta_r + \frac{\chi_r+1}{\chi_r+2}\right)^{\chi_r+1}}{A_r K_{\infty,r}^{(3+\chi_r)}\left(2+\chi_r\right)\left(3+\chi_r\right)\left(1+\beta_r\right)^{\chi_r+2}}\right]^{\frac{1}{\chi_r+1}} \tag{20}$$

EXPERIMENTS ON TWO-BEAM STRUCTURE

The proposed damping model was assessed using experimental measurements on a structure comprised of two beams bolted together. The structure is tested in free-free conditions, and care was taken to design the experimental setup to minimize the effect of damping associated with the boundary conditions. Free boundary conditions were used because any other choice, e.g. clamped, would add even more damping to the system.

Test Structure

In this work, the structure consisted of two beams bolted together with four bolts as shown in Fig. 2. The two beams, each with dimensions 0.508m × 0.051m × 0.006m (20" × 2" × 0.25") were fastened together with 1/4"-28 fine-threaded bolts and all components were made of AISI 304 stainless steel. The bolts were tightened to three different torque levels in these tests: 1.13, 3.39, 5.65 N-m (10, 30, and 50 in-lbs). For reference, the Society of Automotive Engineers (SAE) provides the general torque specification for this type of bolt to be approximately 8.5 N-m (75.0 in-lbs) [12] which results in bolt preload force of approximately 6700 N (1500 lbf). The largest torque used here was somewhat lower than this specification, but, as will be shown, this structure became quite linear for the range of excitation forces that were practical with this setup, so the bolts were kept somewhat loose to accentuate the nonlinearity. Future works will explore methods of exciting the

structure with higher force levels (closer to what might be seen in the applications of interest) so that more realistic torques can be used.

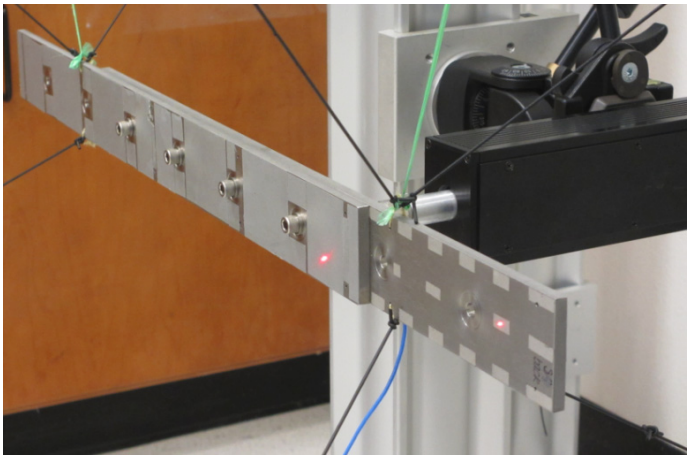

Fig. 2 Photograph of the two beam test structure.

Experimental Setup

The dynamic response of the two beam structure was captured using a scanning laser Doppler vibrometer (Polytec PSV-400), which measured the response at 70 points on the structure. In addition, a single point laser vibrometer (Polytec OFV-534) was used to measure at a reference point to verify that the hammer hits were consistent. The reference laser was positioned close to the impact force location as seen in Fig. 2.

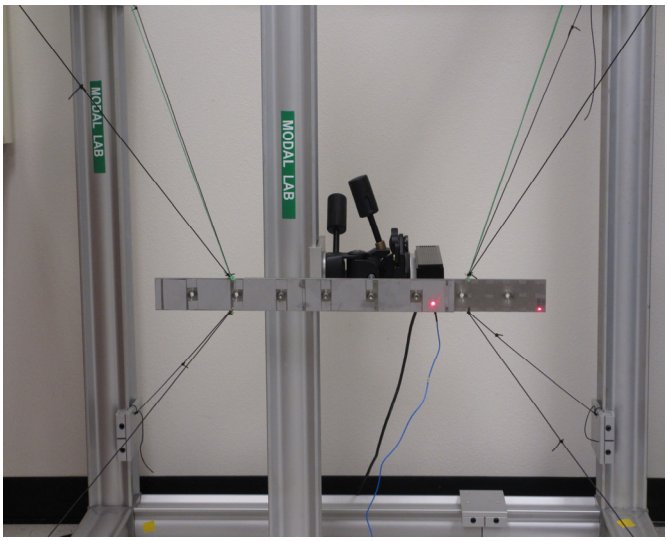

Fig. 3 Photograph of the suspension setup for the two beam test structure.

The structure is suspended by 2 strings that support the weight of the structure and 8 bungee cords which prevent excessive rigid-body motion. The bungees and strings were connected to the beam at locations where the odd bending modes have little motion in order to minimize the damping added to the system.

An Alta Solutions automated impact hammer with a nylon hammer tip was used to supply the impact force, which is measured by a force gauge attached between the hammer and the hammer tip. Additional measurements were taken at higher force levels using a modal hammer; however, the supplied impact force was not as consistent. The mean and standard deviation of the maximum impact force for all of the torque levels and force levels that were used in this study are shown in Table 1.

Table 1: Mean and standard deviation of the maximum impact force for all 70 measurements.

Torque (N-m)	Hammer Level	Mean Impact Force (N)	Standard Deviation of Impact Force (N)
1.13	1 (lowest)	20.24	0.80
1.13	2	32.77	0.27
1.13	3	86.44	0.68
1.13	4 (highest)	288.57	6.10
3.39	1 (lowest)	24.1	0.38
3.39	2	30.9	0.51
3.39	3	52.8	3.84
3.39	4 (highest)	180.1	58.24
3.39	Modal Hammer	1444.5	139.34
5.65	1 (lowest)	20.8	0.44
5.65	2	36.5	0.28
5.65	3	60.3	0.61
5.65	4 (highest)	238.6	15.30
5.65	Modal Hammer	1392.1	172.48

The automatic hammer provides a range of force levels between approximately 20 and 300 N. However, the force level is dependent upon the distance between the hammer tip and the beam and the voltage supplied to the automatic hammer. For these reasons, the lowest and highest force varies for each measurement. For the automatic hammer, the standard deviation tends to increase as the force level is increased. At the highest force level, the automatic hammer has a large spread for all the torque levels especially the 3.39 N-m torque. The modal hammer is able to reach much higher force levels (approximately 1400 N); however, the standard deviations are much larger when compared to the automatic hammer.

Lab Setup Challenges

The damping ratios of a freely supported structure are sensitive to the support conditions, as was explored in detail by Carne, Griffith, and Casias in [13]. Therefore, special attention must be given to the support conditions to assure that the damping that they add does not contaminate the results. Initially, the two beam structures were suspended by two strings that act as pendulum supports as was done in [13]. These support conditions contributed very little damping to the

system; however, several obstacles were encountered with that setup..

Specifically, the velocity of the beam was measured with a scanning laser Doppler vibrometer in order to eliminate any damping associated with the cables that must be added if accelerometers were used. Hence, if the beam swings significantly in its pendulum mode, the point which the laser is measuring may change significantly during the measurement. Also, an automated hammer was used to excite the beam, but the hammer only retracts about 2.5 centimeters (1 inch) after impact. As a result, the pendulum motion of the beam caused almost unavoidable double hits when the bungee cords were not present. Finally, in the processing described subsequently, it is important for the automatic hammer to apply a highly consistent impact force. Any ambient swinging of the beam caused the impact forces to vary from test to test. When the bungee cords were not present, it was extremely difficult and time consuming to try to manually eliminate the ambient swinging. For these reasons, eight soft bungee cords were added to the setup to suppress the rigid body motion of the beam while attempting to add as little stiffness and damping as possible to the system. The final set up was similar to that used in [14] and was shown in Fig. 3. This setup was used for all of the measurements shown in this paper.

A comparison was done to ensure that the addition of bungee cords did not add significant damping to the system. A monolithic structure, without interfaces and bolts, was chosen to ensure that the measured damping was only due to the structure itself and the support conditions. A single beam was suspended with two strings with and without the bungees cords and the damping ratios for the first three modes were found using the Algorithm of Mode Isolation (AMI) [15, 16] and are presented in Table 2.

Table 2: Modal Damping Ratios for a single beam with and without bungees.

Elastic Mode #	ζ without bungees (%)	ζ with bungees (%)
1	0.010	0.016
2	0.025	0.057
3	0.020	0.044

The damping of all of the modes is very light, as one would expect for a monolithic structure. When the bungees were added to the setup, the damping ratios for all modes increased by about a factor of two. The bungees and strings were connected to the beam at locations where the motion of the symmetric or odd bending modes is minimum, to minimize the damping that is added to those modes, but these locations are expected to add some damping to the second mode. However, the results show that the supports added some damping to the first and third modes as well. These damping ratios are an average of the damping ratios found at a range of force levels; the structure is linear so the force level did not have a significant impact on the damping.

Table 3: Averaged Modal Damping Ratios for the two beam test structure.

Elastic Mode #	1.13 N-m Torque, ζ (%)	3.39 N-m Torque, ζ (%)	5.65 N-m Torque, ζ (%)
1	1.2	0.29	0.16
2	0.57	0.48	0.26
3	0.31	0.16	0.11

For comparison, the two beam structure was curve fit to estimate the best fit linear modal damping ratios at each of the three torque levels and the results are presented in Table 3. Due to the nonlinearity introduced by the joints in the two beam structure, the damping ratios seem to change with the amount of excitation applied. The damping ratios presented in Table 3 are an average over all of the data from a range of force levels, and hence they represent a linear fit to a structure which is known to be nonlinear and this probably does introduce some distortion. For each mode, the damping is observed to decrease as the bolt torque increases. This was expected since increasing the bolt torque inhibits micro-slip and hence should decrease the measured damping, although occasionally the opposite has been observed for certain modes [11]. However, even at the tightest bolt torque (5.65 N-m) the modal damping ratios are significantly larger than those in Table 2 for the single beam, by factors of 10, 4.5, and 2.5 for the first three modes respectively. Therefore, it seems that a significant portion of the measured damping is due to the joints in the structure. (The damping in the single beam presumably comes from material damping and the damping provided by the support conditions.)

Lab Data Processing

Two approaches were explored to extract modal velocity ring-downs from the laboratory data. First, mass normalized mode shapes were found by fitting a linear modal model with the Algorithm of Mode Isolation (AMI) [15, 16]. Then the mode shapes were used in a modal filter.

$$\dot{x} = \Phi \dot{q} \tag{21}$$

However, when using a modal filter the modal responses showed clear evidence of frequency content due to other modes, which would contaminate the Hilbert transform analysis. Since this system's modes are well separated, the modes were instead isolated by creating a band pass filter to pass only a single mode, as was done in [11], using a fourth order Butterworth filter. The filtered responses were then divided by the corresponding mass normalized mode shape at each point, *j*, to estimate the modal displacement as, $\dot{q}_r = \dot{x}_j / \Phi_{jr}$. There were 70 measurement points which were then averaged to estimate a single modal velocity for each mode. Some measurement points were excluded from averaging process if the mode was excited too heavily or not

sufficiently. A trimmed mean was used to determine which measurements to keep. The trimmed mean procedure excluded 8 high and low outliers from the set of 70 measurements points. All measurement points whose maximum velocity was within 50 percent of the trimmed mean were kept. The resulting statistics on the filtered impact hammer data are presented in Table 4.

Table 4: Mean and standard deviation of the maximum impact force for the set of measurements that was used.

Torque (N-m)	Hammer Level	Mean Impact Force (N)	Standard Deviation of Impact Force (N)
1.13	1 (lowest)	20.0	0.088
1.13	2	32.8	0.025
1.13	3	86.5	0.041
1.13	4 (highest)	289.3	0.213
3.39	1 (lowest)	24.2	0.013
3.39	2	30.8	0.019
3.39	3	52.7	0.125
3.39	4 (highest)	191.3	1.585
3.39	Modal Hammer	1475.7	3.081
5.65	1 (lowest)	20.9	0.009
5.65	2	36.5	0.005
5.65	3	60.3	0.011
5.65	4 (highest)	237.2	0.310
5.65	Modal Hammer	1400.4	3.225

All of the filtered standard deviations in Table 4 are smaller than the initial standard deviations shown in Table 1. Again, for the automatic hammer, the standard deviation tends to increase as the force level is increased. Yet, at the highest force level, the automatic hammer has a much more reasonable maximum standard deviation of 1.6 N or 0.83%. The modal hammer standard deviations are also improved with a value of approximately 3 N.

In order to compute the model's energy dissipation, a displacement ring-down is needed from the experiment. This was obtained by integrating the measured velocity signal with respect to time using a trapezoidal numerical integration. The displacement ring-down was used to compare the dissipation model (Eq. 6) to the measured experimental data (Eq. 16), as will be shown in Figure 5.

OPTIMIZING MODEL PARAMETERS

The damping parameters $\{F_S, K_T, K_\infty, \chi, \beta, C\}$ of the modal model, seen in Fig. 1, were fit to experimental data using several different optimization routines. The objective function is posed as:

$$\text{Min } f = f_D + f_K \tag{22}$$

where

$$f_D = \left(\frac{D_{Experiment} - D_{Model}}{\max\left(D_{Experiment} - D_{Model} \right)} \right)^2 \tag{23}$$

and

$$f_K = \left(\frac{K_{Experiment} - K_{Model}}{\max\left(K_{Experiment} - K_{Model} \right)} \right)^2 \tag{24}$$

Note that the dissipation and stiffness objective functions, f_D and f_K respectively, are scaled so that their values are on the order of 1.

The nonlinear objective function, Eq. (22), can be optimized using either local or global optimization. Both techniques were explored by the authors in this work; however, when multiple local minima exist, local optimization algorithms tended to be highly dependent on the starting guess. Therefore, a global optimization algorithm (the DIRECT algorithm developed by Jones et al. [17]) was used to provide a more robust approach to optimizing the parameters. In addition, local optimization routines were used in MATLAB (fminsearch, fmincon, lsqnonlin [18]) to fine tune the solution and ensure convergence. Even with the global optimization algorithm, it was important to have a reasonable starting guess. For this work, starting guesses for the $\{F_S, K_T, K_\infty, \chi, \beta\}$ parameters were found using the graphical approach described previously. The initial guess for the modal viscous damping parameter, C, was obtained using the modal damping ratios presented in Table 3 with $C = 2m\zeta\omega_0$.

RESULTS

The measurements from the beam were band-pass filtered and averaged as described previously to isolate the first bending mode of the beam, with the bolts tightened to 3.39 N-m. The optimization procedure was then used to find the modal parameters that best fit the data both with and without the additional viscous damping term. The model without the viscous damper relies entirely on the Iwan joint to dissipate energy. The parameters of the optimized models are shown in Table 5.

Table 5: Optimized parameters of the first bending mode of vibration at a bolt torque of 3.39 N-m, for the modal models with and without the viscous damper.

Parameter	Iwan Model	Iwan & Viscous Damper Model
F_S	6.23	2.33
K_T	$2.61 \cdot 10^5$	$1.37 \cdot 10^5$
K_∞	$3.19 \cdot 10^5$	$4.41 \cdot 10^5$
χ	-0.272	-0.178
β	0.836	0.0316
C	N/A	3.96

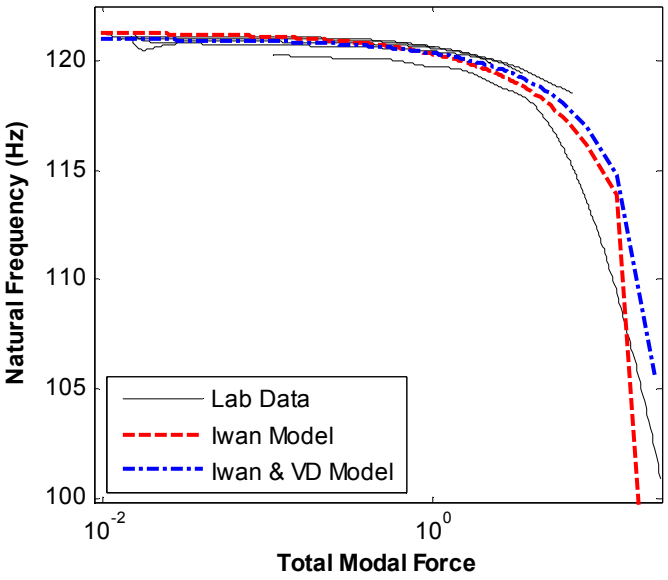

Fig. 4 Comparison between measured natural frequency vs. force and two models.

Fig. 4 shows the natural frequency of the modal Iwan model versus the total modal force for the two modal models, reconstructed using Eq. (7). The measurements show that the natural frequency of this mode changes approximately 20 Hz over the range of forces that were applied. Both models seem to be capable of capturing the change in natural frequency over this range. Unfortunately, the natural frequency is not observed to level off at a frequency ω_∞ as predicted by theory. This suggests that the system never completely reaches macro-slip or that macro-slip is over before the Hilbert transform algorithm is able to capture the macro-slip frequency, making it difficult to estimate the parameters (F_S, K_T, K_∞).

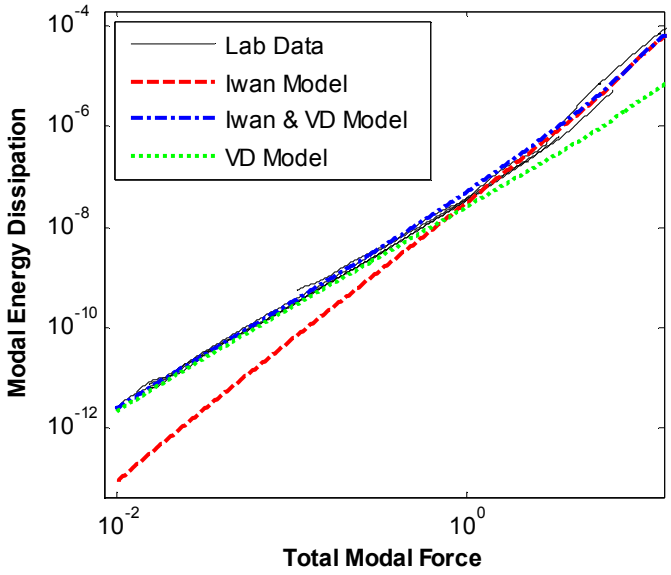

Fig. 5 Energy dissipation comparison of two optimized modal models to experimental data over a range of forces.

Fig. 5 shows the modal energy dissipation versus total modal force for the two modal models and the experimental data at five different excitation levels. The Iwan model without a viscous damper in parallel fails to fit the measurements at low amplitude, while the model with only a viscous damper does not capture the increase in damping at high forces. (Because of the logarithmic scale, the difference at high force levels may appear to be small yet the damping in the linear model is actually in error by an order of magnitude at high energy.) In contrast, the modal Iwan model with a viscous damper in parallel provides an excellent approximation to the measured energy dissipation. It should also be noted that the disagreement between the Iwan model (without a viscous damper) and the measurement at low force levels is not simply due to the choice of parameters. Considerable effort was spent to optimize that model's parameters to better match the measurements, yet the fit could not be improved without decreasing the agreement of the natural frequency versus force plot in Fig. 4. This difficulty disappeared when a viscous damper was added to the model.

The differences between these models is more easily visualized by comparing the slope of the energy dissipation versus force curve. As mentioned previously, a single Iwan joint exhibits a slope of $3+\chi$ on a log dissipation versus log force plot. Fig. 6 compares the slope of the two optimized modal models with the experimentally measured slope. A fifth order polynomial was fit to the laboratory data in order to compute its slope. Without an additional viscous damper, the modal Iwan model has a much larger slope than the laboratory data at low force levels. On the other hand, when a viscous damper is added in parallel with the Iwan joint, the slope follows the laboratory data more closely over the entire range of force levels.

Note that the optimized models have identified a value for the slip force, F_S, that is in the range of the measured forces. Thus, at the highest measured force levels macro-slip has been initiated in both models. Unfortunately, the exciter that was used was not capable of even higher forces so macro-slip could not be fully characterized.

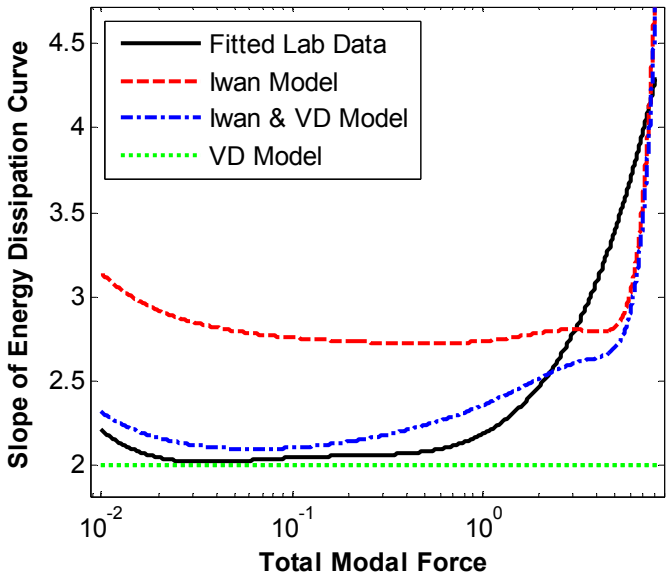

Fig. 6 Slope of energy dissipation versus modal force for modal Iwan models and a polynomial fit to the experimental measurements.

This same procedure was repeated for the first three elastic modes at three different bolt torques and the identified modal Iwan parameters are shown in Table 6. Only the first three elastic modes were analyzed in this work due to the lack of response from the higher frequency modes. The last two rows of each section of Table 6 give the natural frequency and modal damping ratio, which can be readily computed from the other parameters.

Table 6: Optimized parameters for a modal Iwan model with a viscous damper. First three elastic modes each at varying bolt torques.

Bolt Torque N-m (in-lbf)	1.13 (10)	3.39 (30)	5.65 (50)
1st Elastic Mode			
F_S	0.562	2.33	3.08
K_T	$1.16\cdot10^5$	$1.37\cdot10^5$	$1.35\cdot10^5$
K_∞	$5.03\cdot10^5$	$4.41\cdot10^5$	$4.44\cdot10^5$
χ	-0.0237	-0.178	-0.0102
β	0.0237	0.0316	1.19
C	1.89	3.96	1.12
f_0 (Hz)	125.2	121.0	121.1
ζ (%)	0.120	0.099	0.074
2nd Elastic Mode			
F_S	1.10	27.0	27.34
K_T	$1.61\cdot10^5$	$5.10\cdot10^5$	$4.08\cdot10^5$
K_∞	$1.80\cdot10^6$	$1.31\cdot10^6$	$1.40\cdot10^6$
χ	-0.195	-0.310	-0.303
β	0.000458	0.523	3.80
C	5.62	15.11	5.69
f_0 (Hz)	222.9	214.7	214.0
ζ (%)	0.201	0.560	0.216
3rd Elastic Mode			
F_S	6.77	5.26	23.04
K_T	$1.45\cdot10^6$	$1.36\cdot10^6$	$2.79\cdot10^6$
K_∞	$7.15\cdot10^6$	$7.50\cdot10^6$	$6.39\cdot10^6$
χ	-0.112	-0.228	-0.0196
β	1.46	5.94	13.68
C	11.8	2.96	4.18
f_0 (Hz)	466.7	473.7	482.2
ζ (%)	0.201	0.050	0.069

The results above show that the slip force parameter, F_S, tends to increases when the bolts are tightened for all modes considered. This is as expected since, ass the bolts are tightened, the preload in the bolts increases so larger forces are required to initiate macro-slip. As the bolts are tightened, one would expect that the K_∞ parameter for each mode would stay relatively constant while the joint stiffness, K_T, would increase. However, the optimized stiffness parameters, K_T and K_∞, seem not to follow much of a trend for this system. This probably indicates that the measured data is not adequate to reliably estimate K_∞, as might be expected since the excitation force was not sufficient to bring the system well into macro-slip. The joint parameter, χ, can be observed to decrease as the bolt torques are increased from 1.13 to 3.39 N-m. This is to be expected, since the energy dissipation resembles a linear system at high bolt torques. However, from 3.39 to 5.65 N-m the χ parameter increases. This means the energy dissipation of the Iwan model has become more nonlinear to account for the slip region that contains a great deal of energy dissipation close to the macro-slip region. Finally, the viscous damping parameter, C, seems to remain in a similar range for each mode considered. The equivalent low-amplitude damping ratio is also shown and these damping ratios are comparable to those in Table 3 and hence they seem to be plausible lower bounds for the damping in the system, due the supports and material damping.

Validating the Modal Model

The optimized modal model from Table 6 was next validated by comparing the response of the nonlinear model with an experimentally measured response. The response at the midpoint of the 2 beam set up was selected for the location of interest. The bolts of the 2 beam structure were tightened to 3.39 N-m and an impact force with a maximum value of approximately 53 N (or the 3rd force level from Table 1 and Table 4) was applied to the structure using the automatic

hammer. The experimentally measured impact force was used as an input and the modal equations of motion for each of the modes (using the parameters in Table 6) were integrated in time with a Newmark-Beta time integration routing with a Newton-Raphson iteration loop for the nonlinear force in the Iwan model. The response at the midpoint of the beam was then found by adding the contribution of each mode and using the mass normalized mode shapes.

The responses were first compared in the frequency domain where it was easy to ignore the effect of the rigid body modes. In addition, a zeroed early-time fast Fourier transform (ZEFFT) [3] was used to show how the nonlinearity of both the model and the measured data progressed over time. Fig. 7 shows the ZEFFTs taken at several different times including: 0.051, 0.29, 0.53, 0.76, and 1.0 second as indicated in the legend. The solid and dashed lines correspond to the experimentally measured response and the simulated response from the modal Iwan models respectively.

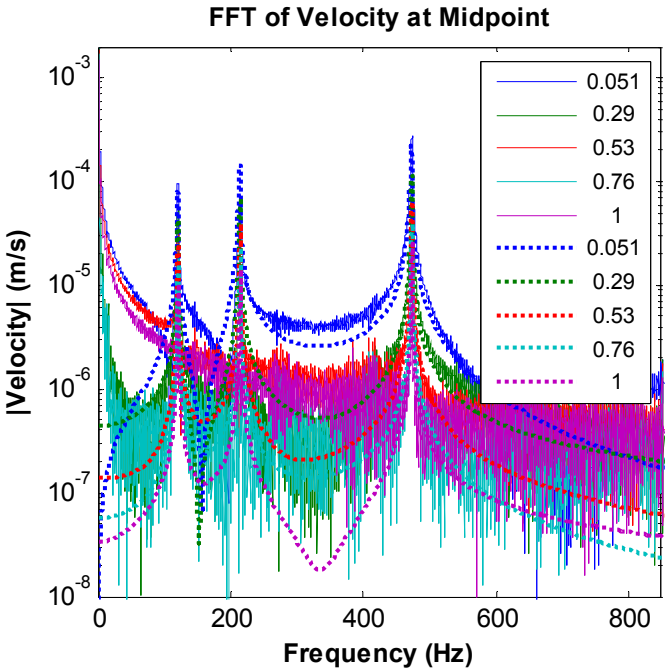

Fig. 7 ZEFFTs for the midpoint of the structure for both the experimental measurement (solid lines) and the model (dashed lines).

The ZEFFTs show that the first three modes dominate the response in this frequency range and that the frequencies do not shift very much over time. The model matches the measurement very well, except at those frequencies where the measurement falls below the noise floor of the sensors. It is typically necessary to zoom in near each resonance peak to evaluate the ZEFFTs for a system such as this. Fig. 8 shows a zoomed in view of the first resonant peak from Fig. 7. This comparison reveals that the model agrees quite well with the measurements; both predict a similar variation in the amplitude of the peak with time and a similar level of smearing as the frequency of oscillation increases with time (due to decreasing amplitude). It is important to note that no filtering was performed on the measured data, so this confirms that the filters used when obtaining the modal Iwan parameters have not distorted the data significantly.

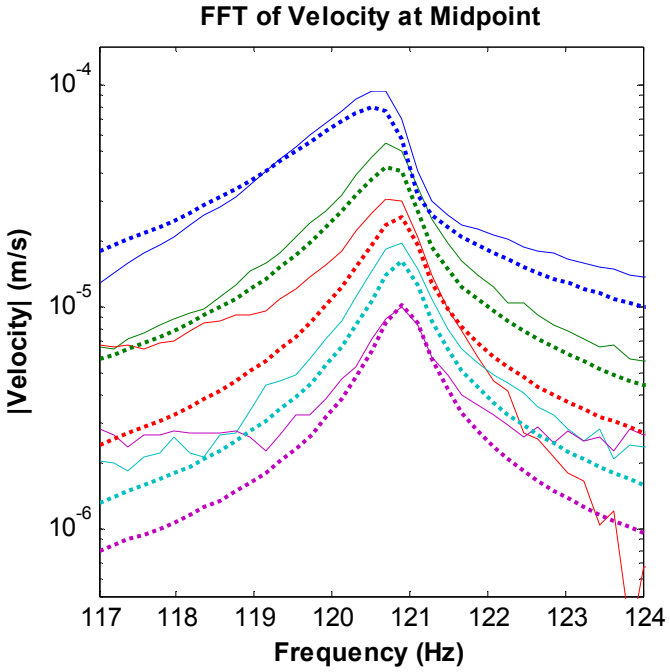

Fig. 8 Zoomed in view of the first resonant peak with ZEFFTs for the both the experimental measurement (solid lines) and the model (dashed lines).

In order to compare the responses in the time domain, a filter was applied to eliminate the rigid body motion. The measured response was filtered using a fourth order Butterworth filter, with frequencies between 50 and 600 Hz kept. Note that other frequency bands were experimented with and including higher frequencies in the filtering process did not change the time response significantly. The filtered measured response was compared to the simulated response in the time domain as shown in Fig. 9.

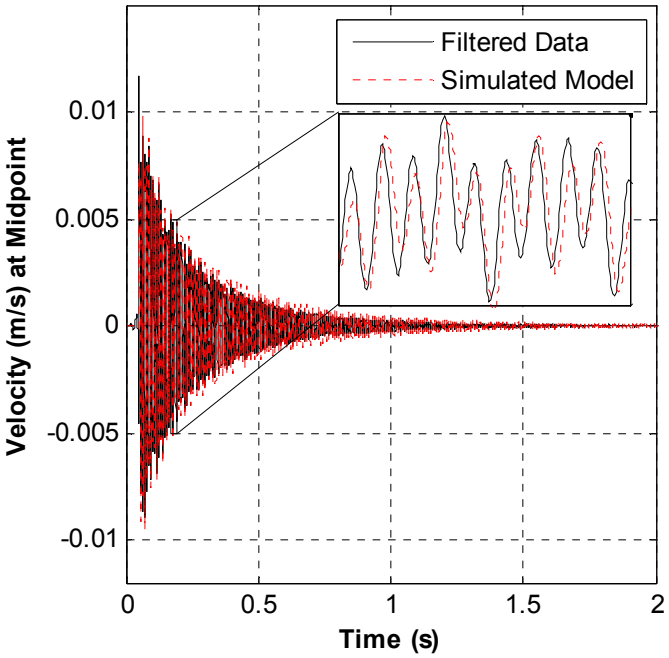

Fig. 9 Time response comparison of the filtered experimental measurement (solid lines) and the model (dashed lines).

The velocity ring-down for the model (dashed line) is observed to compare very well with the ring-down of the filtered measurement (solid line). In this type of comparison, it is important to note that the measured data is filtered which could distort the signals, but in this case the distortion would hopefully be minimal since only the rigid body motions have been eliminated.

CONCLUSION

In this work, a viscous damper was added in parallel with a modal Iwan model and a procedure was discussed to identify parameters for the model from laboratory data. The 4-parameter Iwan model was found to fit the measurements very well for the first three bending modes, suggesting that modal coupling was weak and that a modal Iwan model may be an effective way of accounting for the nonlinear damping associated with the mechanical joints of the system. The measurements also showed that it was important to also have a viscous damper in parallel with the Iwan element in order to account for the linear damping associated with the material and the boundary conditions. There are only a few parameters to identify and the parameters χ, β, C and K_T are all fairly clearly represented in the modal response. On the other hand, in this study F_S and K_∞ were somewhat difficult to estimate since we were not able to apply large enough input forces to drive the system well into the macro-slip regime. This is likely to always be a problem when impulsive forces are used since the joint dissipates a lot of energy in the first few cycles, before the filters and Hilbert transform have stabilized.

This modal Iwan approach is very appealing since it allows one to treat a structure as a set of uncoupled linear modes with slightly nonlinear characteristics in the micro-slip regime; a collection of modal Iwan models such as this is extremely inexpensive to integrate, making this approach very attractive whenever the force levels are low enough that the approach is sufficiently accurate. In the validation section, this model was used to predict the response of the structure to a measured impulsive force and the comparison showed that the modal Iwan model did accurately predict the measured response over the frequency range of interest. Future works will further explore the validity of the modal model, by using inputs at other locations and other types of inputs. To date, experimental and analytical results have suggested that this approach can be very successful, except perhaps at very high force levels when serious macro slips occur [6].

ACKNOWLEDGMENTS

The experimental work for this paper was conducted at Sandia National Laboratories. Sandia is a multi-program laboratory operated under Sandia Corporation, a Lockheed Martin Company, for the United States Department of Energy under Contract DE-AC04-94-AL85000. The authors would especially like to thank Jill Blecke, Hartono Sumali, Randall Mayes, Brandon Zwink and Patrick Hunter for the help that they provided with the laboratory setup and testing.

REFERENCES

[1] D. J. Segalman, "An Initial Overview of Iwan Modelling for Mechanical Joints," Sandia National Laboritories, Albuquerque, New Mexico SAND2001-0811, 2001.

[2] D. J. Segalman, "A Four-Parameter Iwan Model for Lap-Type Joints," *Journal of Applied Mechanics,* vol. 72, pp. 752-760, September 2005.

[3] M. S. Allen and R. L. Mayes, "Estimating the degree of nonlinearity in transient responses with zeroed early-time fast Fourier transforms," *Mechanical Systems and Signal Processing,* vol. 24, pp. 2049-2064, 2010.

[4] D. J. Segalman and W. Holzmann, "Nonlinear Response of a Lap-Type Joint using a Whole-Interface Model," presented at the 23rd International Modal Analysis Conference (IMAC-XXIII), Orlando, Florida, 2005.

[5] D. J. Segalman, "A Modal Approach to Modeling Spatially Distributed Vibration Energy Dissipation," Sandia National Laboratories, Albuquerque, New Mexico and Livermore, California SAND2010-4763, 2010.

[6] B. J. Deaner, M. S. Allen, M. J. Starr, and D. J. Segalman, "Investigation of Modal Iwan Models for Structures with Bolted Joints," presented at the

International Modal Analysis Conference XXXI, Garden Grove, California USA, 2013.
[7] Q. Zhang, Allemang, R. J. , Brown, D. L., "Modal Filter: Concept and Application," presented at the 8th International Modal Analysis Conference (IMAC VIII), Kissimmee, Flordia, 1990.
[8] S. D. Stearns, *Digital Signal Processing with Examples in Matlab*. New York: CRC Press, 2003.
[9] M. Feldman, "NON-LINEAR SYSTEM VIBRATION ANALYSIS USING HILBERT TRANSFORM - I. FREE VIBRATION ANALYSIS METHOD 'FREEVIB'," *Mechanical Systems and Signal Processing,* vol. 8, pp. 119-127, 1993.
[10] H. Sumali and R. A. Kellogg, "Calculating Damping from Ring-Down Using Hilbert Transform and Curve Fitting," presented at the 4th International Operational Modal Analysis Conference (IOMAC), Istanbul, Turkey, 2011.
[11] M. W. Sracic, M. S. Allen, and H. Sumali, "Identifying the modal properties of nonlinear structures using measured free response time histories from a scanning laser Doppler vibrometer," presented at the International Modal Analysis Conference XXX, Jacksonville, Florida USA, 2012.
[12] S. M. Dickinson, "On the Use of Simply Supported Plate Functions in Raleigh's Method Applied to the Flexural Vibration of Rectangular Plates," *Journal of Sound and Vibration,* vol. 59, pp. 143-146, 1978.
[13] T. G. Carne, D. T. Griffith, and M. E. Casias, "Support Conditions for Experimental Modal Analysis," *Sound and Vibration,* vol. 41, pp. 10-16, 2007.
[14] H. Sumali, "An experiment setup for studying the effect of bolt torque on damping," presented at the 4th International Conference on Experimental Vibration Analysis for Civil Engineering Structures (EVACES), Varenna, Italy, 2011.
[15] M. S. Allen and J. H. Ginsberg, "A Global, Single-Input-Multi-Output (SIMO) Implementation of The Algorithm of Mode Isolation and Applications to Analytical and Experimental Data," *Mechanical Systems and Signal Processing,* vol. 20, pp. 1090-1111, 2006.
[16] M. S. Allen and J. H. Ginsberg, "Global, hybrid, MIMO implementation of the algorithm of mode isolation," in *23rd International Modal Analysis Conference (IMAC XXIII)*, 2005.
[17] D. R. Jones, Perttunen, C. D., Stuckman, B. E., "Lipschitzian Optimization Without the Lipschitz Constant," *Journal of Optimization Theory and Application,* vol. 79, pp. 157-181, 1993.
[18] "Optimization Toolbox For Use with MATLAB," ed. Natick, MA: The MathWorks, Inc., 2003.